Polímeros
ISSN 1678-5169 (Online)

https://doi.org/10.1590/0104-1428.20230062

ORIGINAL ARTICLE

Effect of accelerated weathering environment on the carbon fiber/polyamide 6 composites

Larissa Stieven Montagna[1]*, Guilherme Ferreira de Melo Morgado[1], Juliano Marini[2], Thaís Larissa do Amaral Montanheiro[3], Alessandro Guimarães[4], Fabio Roberto Passador[1] and Mirabel Cerqueira Rezende[1]

[1] Laboratório de Tecnologia de Polímeros e Biopolímeros – TecPBio, Universidade Federal de São Paulo – UNIFESP, São José dos Campos, SP, Brasil

[2] Departamento de Engenharia de Materiais, Universidade Federal de São Carlos – UFSCar, São Carlos, SP, Brasil

[3] Departamento de Engenharia Mecânica, Instituto Tecnológico de Aeronáutica – ITA, São José dos Campos, SP, Brasil

[4] Laboratório de Estruturas Leves – LEL, Instituto de Pesquisas Tecnológicas do Estado de São Paulo – IPT, São José dos Campos, SP, Brasil

**larissa.s.montagna@gmail.com*

Abstract

Prolonged exposure to environmental conditions such as ultraviolet radiation, humidity, and temperature, to which carbon fiber-reinforced thermoplastic polymer components are exposed during their service life, can lead to significant changes in mechanical, physical, and chemicals properties, and can often be irreversible, resulting in premature component failure. This study presents the influence of accelerated weathering exposure times (400 h, 800 h, and 1200 h) on the mechanical, thermal, and structural properties of carbon fiber (CF)/polyamide 6 (PA6) laminates. Analyses of composite surfaces were carried out using microscopy and contact angle measurements, which indicated that the factors of exposure to accelerated only affected the surface of the composites, showing signs of the beginning of degradation. The tensile strength (609 MPa ± 10 MPa) and interlaminar shear strength (27 MPa ± 0.9 MPa) did not present significant changes, showing that the reinforcement, the matrix, and the interface remained stable after exposure to accelerated.

Keywords: *accelerated weathering, carbon fiber, composites, polyamide 6, ultraviolet radiation.*

How to cite: Montagna, L. S., Morgado, G. F. M., Marini, J., Montanheiro, T. L. A., Guimarães, A., Passador, F. R., & Rezende, M. C. (2023). Effect of accelerated weathering environment on the carbon fiber/polyamide 6 composites. *Polímeros: Ciência e Tecnologia*, *33*(3), e20230032. https://doi.org/10.1590/0104-1428.20230062

1. Introduction

Carbon fiber reinforced thermoplastic polymer (CFRTP) has proven to be an excellent replacement option for traditional carbon fiber composites with thermoset resins due to its good mechanical properties, such as high strength and rigidity, easy and fast processing, in addition to the possibility of being recycled at the end of its useful life[1,2]. CFRTP has been widely used in sectors that demand lightweight structural applications, such as aerospace[3], automotive[4,5], renewable energies[6], and sports goods[7].

During their lifespan, CFRTPs are exposed to the most aggressive environmental factors, such as humidity, temperature gradients, solar radiation, ozone, pollution, mechanical factors load, and some chemical products, that individually or in combination, may affect their thermal, chemical, and mechanical properties, resulting in a decrease in service life[8]. Among these factors, changes in temperature, humidity, and ultraviolet (UV) radiation prevail. According to Sang et al.[9], the variation in "hot/humid" exposure to which CFRTPs are often subjected during the working period is considered the most severe condition in terms of degradation. Aiming at increasing its useful life, therefore, it is crucial to understand the behavior of the diffusion and damage characteristic of CFRTP when subjected to environmental exposure.

UV radiation from sunlight also affects polymer composites, as the energy of UV photons is similar to the covalent bonds of polymeric materials, thus it can affect and alter the chemical structure of polymeric chains[10,11]. The depth of UV radiation penetration is small, in the order of micrometers. The reinforcement of carbon fiber (CF) in composite materials absorbs and limits the penetration of UV radiation, resulting in the superficial degradation of the composite[12].

However, this phenomenon can lead to the formation of small flaws and surface cracks, which facilitate the penetration and diffusion of moisture and pollutants into the composite. These factors can be intensified with the

increase in temperature, and in this way, they can act as stress concentrators, and lead to the formation of surface tensions, which, when accumulated, generate stress. This stress may propagate to the interior of the thermoplastic composite, resulting in the formation of cracks, in addition to premature failure during the life of the component[13,14].

Among the engineering thermoplastics, polyamide 6 (PA6) has been highlighted due to the ease of processing and the fact that CF/PA6 composite laminates can be prepared using the same equipment used to prepare thermoset resin laminates. PA6 is a thermoplastic composed of amide monomers connected by peptide bonds, with good resistance to impact, abrasion, and wear, good mechanical stability, and high resistance to chemical and biological attacks, in addition to being extremely rigid and resistant up to 180 ºC[15]. However, PAs can undergo different degradation processes due to their highly hygroscopic nature, and the presence of moisture results in degradation by hydrolysis of the amide, which can be accelerated with the presence of temperature[16]. The influence of UV radiation combined with oxygen and temperature results in photo-oxidative, and thermo-oxidative degradation, respectively, causing polymer chain scission, micro-cracking, discoloration due to the production of chromophoric chemical species, the opacity of the polymer surface, and consequently a significant loss in the mechanical properties[17,18].

CF is widely used to reinforce polymeric materials, to be applied in different sectors. CF has good chemical stability and high heat resistance, in addition to absorbing little or no moisture, so it has been used as reinforcement in PA6 matrices to minimize or even delay the effects of weathering conditions of the polymeric matrix[1,19-21]. In addition to improving resistance and mechanical, thermal, and chemical stability. Pinpathomrat, Yamada, and Yokoyama[22] studied the effect of ultraviolet-C (UV-C, 20.2 W/m^2) irradiation on neat PA6 and CF/PA6 composites, and observed a drastic decrease in tensile strength in neat PA6, while for CF/PA6 composite no major changes were observed, indicating that CF is useful not only as composite reinforcement but also for UV protection of PA6.

The present work aims at determining the influence of accelerated weathering, including rain cycles, temperature, and UV radiation using a weather meter machine, on the mechanical (tensile strength and interlaminar shear strength) and thermal (melting temperature and degree of crystallinity) properties, and morphological characteristics by optical microscopy (MO) and scanning electron microscopy (SEM) of CF/PA6 composites. CF/PA6 composite laminates are used to manufacture lightweight outdoor structures for the automotive and oil and gas industries. These composites are subjected to climate and environmental change that include the presence of humidity and UV radiation. Therefore, the degradation of polymers-based composite components and/or structures must be taken into account, aiming at the safety of human health and the environment.

2. Materials and Methods

2.1 Materials and specimens cutting

The thermoplastic composite used is polyamide 6 reinforced with carbon fiber (CF/PA6) 5 plies, 2x2 twill carbon fiber weave, 415 gsm, and 39 wt% matrix content (Cetex® TC910) from Toray® Advanced Composites Co. (England). The material was used as received. The cutting of the standardized specimens for the mechanical test (tensile test and ILSS) was carried out in a cutting machine (Extec Corp., LAbcut 5000) with a cutting speed of 2 mm/s.

2.2 Accelerated weatherometer

The CF/PA6 composite samples were placed in a UV test fluorescent UV/condensation weathering instrument (Atlas, 22007) with a UV test radiometer (Atlas, 24078), using UVA-340 lamps with 0.89 W/m^2 of irradiation intensity, with a cycle of 8 h of UVA irradiation at a temperature of 60 ºC (± 3 ºC), intercalated with 4 h of condensation at a temperature of 50 ºC (± 3 ºC). These factors were submitted on both sides of the composite samples, to homogenize and standardize the effects. The CF/PA6 composite specimens were subjected to UV radiation and were removed at 400 h, 800 h, and 1200 h (on both sides), then were tested and evaluated.

Text paragraph within a second subsection.

2.3 Characterizations

The contact angle measurements were performed in a Goniometer Ramé-Hart (model 500), and the liquid used was distilled water by the sessile drop method (1.0 μL, 25 °C). Nine measurements were made in each sample to evaluate the surface character of the CF/PA6 composites unexposed and after 400 h, 800 h, and 1200 h exposed to accelerated weathering.

Fourier-transformed Infrared Spectroscopy (FT-IR) measurements of CF/PA6 composites before and after 400 h, 800 h, and 1200 h exposed to accelerated weathering were carried out in a PerkinElmer spectrometer (model 2000) using universal attenuated total reflectance (UATR), with an average of 20 scans with 2 cm^{-1} resolution, in the range from 4000 to 500 cm^{-1}.

DSC analyses of CF/PA6 composites unexposed and after 400 h, 800 h, and 1200 h exposed to accelerated weathering were performed using TA Instruments equipment (Q2000 model) in an inert nitrogen atmosphere (50 mL/min). The samples were heated from 30 °C to 300 °C, with a heating rate of 10 °C/min, with 3 min isotherm, at 300 °C, to eliminate the thermal history of the samples, and after that, they were cooled and heated again from 300 °C to 30 °C at a rate of cooling and heating of 10 ºC/min. The degree of crystallinity (X_c, %) was determined by Equation 1, where ΔH_m is the enthalpy of melting of the semicrystalline PA6 and ΔH_{CC} is the enthalpy of cold crystallization (ΔH_{CC} = 0 J/g, in this case), both according to the result of DSC analysis from the 2nd heating. Θ is the carbon fiber mass fraction in the composite (according to Montagna et al.[23] this CF/PA6 composite has 51% CF), and ΔH_m^0 is the enthalpy of melting of the 100% crystalline polymer (ΔH_m^0 = 230 J/g for PA6[24]).

$$Xc = \frac{(\Delta H_m - \Delta H_{cc})}{(1-\theta)\Delta H_m^0} \times 100 \quad (1)$$

Tensile tests were carried out according to ASTM D3039[25] using an Instron (model 5982), with sample dimensions of

250 mm x 25 mm x 2.3 mm (length x width x thickness), and a crosshead speed of 2 mm.min^{-1} and load cell of 250 kN. Seven specimens of each sample were tested.

The interlaminar shear strength (ILSS) by short beam method was performed to evaluate CF interfacial adhesion mechanisms with the PA6 matrix. The samples (24 mm x 6.35 mm x 4.0 mm) were performed with a 100 kN load cell on an Instron (model 5982) and a testing speed of 1.0 mm/min, according to ASTM D2344[26]. For this purpose, six specimens were tested for each case studied. The interlaminar shear strength (τ_{max}) was calculated by dividing the peak recorded reaction force (P) by the area of the cross-section ($b\,x\,h$), as shown in Equation 2.

$$\tau_{max} = 0.75\frac{P}{(b\,x\,h)} \quad (2)$$

Mechanical test results were analyzed using one-way analysis of variance (ANOVA) and Tukey's multiple comparisons test on GraphPad Prism 6 (GraphPad Prism 6 Software Inc. USA) at 95 and 99.9% levels, respectively.

The fractured surface after the ILSS test was performed through images obtained by optical microscopy (OM) using a benchtop optical microscope (MP-150). Surface degradation and the fractured surfaces of specimens after tensile tests were analyzed by scanning electron microscopy (SEM) with a scanning electron microscope Inspect S50 (FEI Company®) at an accelerating voltage of 20 kV. The CF/PA6 composite samples were placed in the aluminum stub with carbon tape and coated with a thin layer of gold for 120s[27], by sputtering from Quorum (Q150RS Plus).

3. Results and Discussions

The quantification of moisture absorption by the specimens after accelerated weathering did not show a significant increase in the weight gain of the samples. This behavior is attributed to the intercalated cycles of wet (water at 50 ºC) and dry (UV irradiation at 60 ºC), which maintained the weight of the specimens around the initial value before conditioning. Although the specimens did not show moisture absorption at the end of conditioning, the possible influence of the accelerated weathering on the composites was investigated by FT-IR and thermal analyses.

Figure 1 shows the structural changes of CF/PA6 composite surfaces before and after 400 h, 800 h, and 1200 h in accelerated weathering measured by FT-IR. All the spectra are very similar, occurring a reduction of insignificant intensities of the bands or their displacement. That is, insignificant chemical degradation was observed by FT-IR on the surface of CF/PA6 after conditioning in an accelerated weathering by small changes in the carbonyl area and hydrolysis.

The photooxidation of the surface of CF/PA6 composites can be monitored mainly by the appearance of a band around 1715 cm^{-1}, corresponding to the stretching of the carbonyl, referring to the possible oxidation of the matrix that occurred after the process of exposure to UV radiation; and by changes in the intensity of the bands at 3000–3500 cm^{-1} referring to alcohols and carboxylic acids[28]. In none of the spectra shown in Figure 1-A was observed the band around 1715 cm^{-1}. However, an increase in the intensity of the band at 3300 cm^{-1} was observed in the exposed CF/PA6 composite at 1200 h, which may be due to moisture absorption during the periods of wet conditioning to which it was subjected[29]. The occurrence of degradation by hydrolysis can be indicated through the reduction in the amide band (1633 cm^{-1} and 1540 cm^{-1}) intensities after the conditioning test suggesting that the amide was degraded[30]. This behavior was observed in the composites after the exposure time of 400 h and 800 h.

To evaluate the degradation of the samples exposed to accelerated weathering, the ratio between interest bands was calculated, since there is a change in their intensities proportionally to the concentration of these groups (Figure 1-B). Once the degradation can be monitored by the change in intensity of the amide band, the ratios 3300/1633 and 3300/1540 were obtained. Whereas the degradation by hydrolysis is indicated by the reduction in amide band intensity, is expected that, for samples that were degraded, the ratio between 3300/1633 and 3300/1540 bands increases if compared to the unconditioned sample. Figure 1-B shows the ratios between bands for all samples. It can be concluded that after 1200 h of accelerated weathering the sample presented degradation of the amide band. After 400 h and

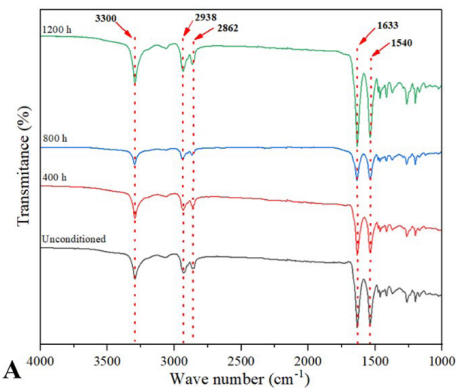

B

Samples	Ratio		
	3300/1633	3300/1540	1633/1540
Unconditioned	1.35	1.32	0.98
400 h	1.27	1.24	0.98
800 h	1.08	1.07	0.99
1200 h	1.64	1.50	0.92

Figure 1. FT-IR results: spectra (A) and the results of the ratio between interest bands (B) of CF/PA6 composites before and after the exposure times of 400 h, 800 h, and 1200 h in accelerated weathering.

800 h, the reduction in the ratios may be justified by some water adsorption of samples. To confirm the degradation, the ratio between both amide bands was also calculated; seeing that, a variation in this ratio indicates that the functional groups were somehow affected. The 1633/1540 ratios were nearly the same for unconditioned, 400 h and 800 h samples, but for 1200 h showed variation, confirming the matrix degradation of this sample.

The thermal properties of samples exposed to accelerated weathering were evaluated using DSC and aimed to verify the influence of different exposure times (400 h, 800 h, and 1200 h) on the melting temperature (T_m) and degree of crystallinity (X_c). Figure 2 presents the DSC curves in the first and second heating. It is possible to observe in the DSC curves referring to the first heating that the composites did not present significant changes in the value of the T_m, and all composites presented T_m values at approximately 217 ºC (± 0.5 ºC). However, when checking the curves for the second heating, the presence of a double endothermic peak in the T_m region is noticeable, with T_{m1} at approximately 214 ºC ± 0.8 and T_{m2} at 218.8 ºC ± 0.5 ºC. The presence of these double peaks in crystalline melting could be due to different crystalline forms, α phase, and γ phase. The α phase is considered the most stable and predominant, and the γ phase is less stable and is formed by rapid cooling. A similar behavior was observed in the study carried out by Oulidi et al.[31].

Also, through the DSC analysis, it was possible to verify a slight difference in the composites after the different exposure times to the accelerated weathering chamber. Increases of 21%, 26%, and 13% in the X_c values of the CF/PA6 composites after 400 h, 800 h, and 1200 h exposure to accelerated weathering, respectively, when compared to the unconditioned composites were observed. This increase may be related to the breaking of intramolecular bonds and the reorganization of the polymeric chains, associated with the crystalline regions that were influenced by the environmental factors to which they were exposed, such as UV radiation, humidity, and temperature. These factors influenced the increase of the crystalline phase. Similar behavior was observed by Mahat et al.[32], who observed that as the exposure time of CF-reinforced thermoplastic composites increased, crystallinity values increased, as the molecular structure becomes more ordered with increasing crystallinity and consequently restricts the movement of the amorphous region.

Figure 3 shows the results obtained in the mechanical characterization of unconditioned specimens and those exposed to accelerated weathering. Figure 3-A-B shows the results of the ultimate tensile strength (UTS) and elastic modulus (E) of the CF/PA6 composites unconditioned and after 400 h, 800 h, and 1200 h exposed to accelerated weathering. Through the analysis of variance (ANOVA) and Tukey's multiple comparisons tests, no statistical difference was observed in the results of the analyzed mechanical properties.

In Figure 3-A, it is possible to observe that the periods of 400 h, 800 h, and 1200 h of accelerated weathering exposure did not cause a significant effect on the UTS values, since all values are within the standard deviation range. Furthermore, this property is governed by the fiber and not by the polymeric matrix, which is more susceptible to degradation, preserving the reinforcement. It is worth remembering that the moisture absorption by the specimens at the end of the accelerated weathering conditioning was not significant, due to the alternating cycles with and without humidity, which favored that the moisture absorbed during the wet cycle was lost during the dry cycle. Thus, the tensile strength and elastic modulus were not significantly affected by the accelerated weathering exposure, as related in the literature for CF-reinforced composites[33].

Figure 3-C shows the UTS *vs* X_c curve of specimens unconditioned and exposed to different times of conditioning. This Figure 3-C shows the increase of X_c with the time of exposure in the accelerated weathering about the unconditioned specimen but without a consistent correlation with the UTS values, considering that the variation of this property has no statistical difference according to ANOVA and Tukey's multiple comparisons. The X_c behavior may be due to structural changes caused by increased exposure, which may be related to a possible restructuring of the molecular chains, altering the degree of crystallinity and/or by the adsorbed humidity which makes greater the free volume among the chains. According to the literature[34], the stiffening of the material can be increased with the X_c increase. In the present study, the combined factors of UV radiation, humidity, and

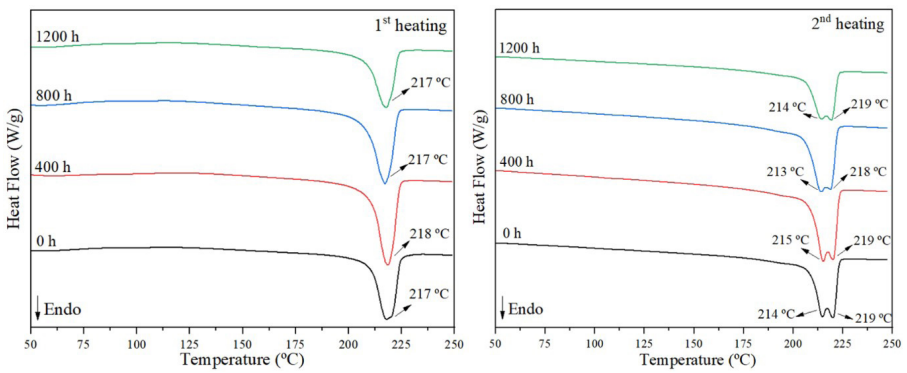

Figure 2. DSC curves from 1st and 2nd heating of CF/PA6 composites unconditioned and after 400 h, 800 h, and 1200 h exposed to accelerated weathering.

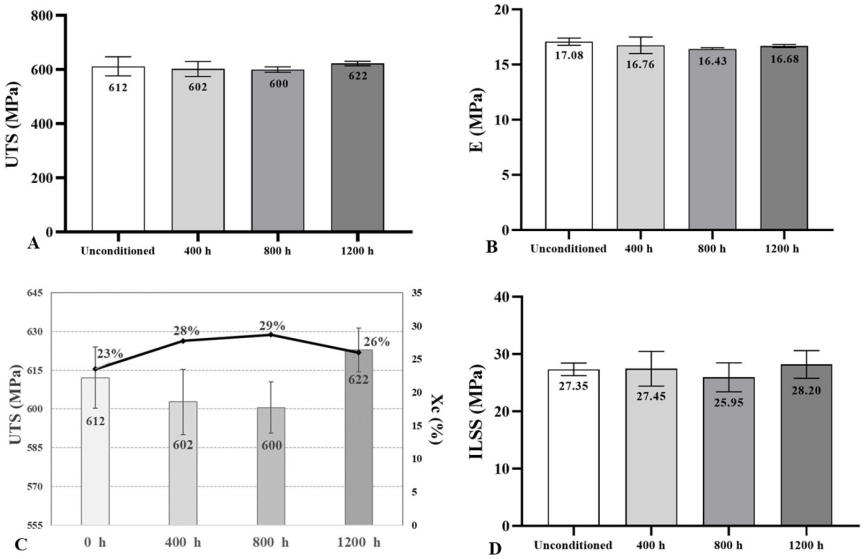

Figure 3. CF/PA6 composites unconditioned and after 400 h, 800 h, and 1200 h exposed to accelerated weathering: ultimate tensile strength, UTS (A), elastic modulus, E (B), UTS *vs* X_c (C), and interlaminar shear stress, ILSS (D).

temperature may have promoted a slight increase in the UTS property, as observed for the composite after 1200 h of exposure, which presented a slight increase of 1.6%, when compared to the unconditioned composites.

As for the elastic modulus values (Figure 3-B), a reduction of approximately 2.7% (± 1%) was observed in the composites after different exposure periods in accelerated weathering, when compared to the unconditioned composite, probably due to the small amount of the absorbed humidity.

Figure 4 shows representative macroscopic images of the UTS fracture of the CF/PA6 composites, unconditioned and after exposure to accelerated weathering. The images of the unconditioned composites (Figure 4-A-B-C) are typical of tensile fracture with total rupture of the specimen, with CF and matrix fracture, and consequently translaminar, intralaminar, and interlaminar fractures and more extensive delaminations. In the images of the composites after 400 h of exposure to accelerated weathering (Figure 4-D-E-F), it is possible to visualize the partial rupture of the specimen (Figure 4-D), with the rupture of CFs and with several intralaminar, interlaminar, and translaminar fractures. The images referring to the composites after 800 h (Figure 4-G-H-I) and 1200 h (Figure 4-J-K-L) after exposure to accelerated weathering show a more severe rupture, with the combination of intralaminar, interlaminar, and translaminar fractures, and fiber failure with aspects similar to those observed in compression failures, plus wedge split fault (highlighted with a green rectangle, in Figure 4-G and K).

Prolonged exposure to UV radiation, humidity, and temperature can contribute to the degradation of the polymeric matrix, affecting the properties that are governed by the matrix, as is the case of ILSS. Therefore, through the analysis of the ILSS (Figure 3-D), it was possible to verify the adhesion between the CF and the matrix, in addition to the analysis of the interfacial failure, which allows evaluating the integrity of the interface that is a prerequisite for a good stress transfer in the laminate. In this way, the ILSS test allowed evaluation of the quality and integrity of the interface between the PA6 matrix and the CF of the composites after 400 h, 800 h, and 1200 h exposed to accelerated weathering, and the OM images (Figure 5) assisted in assessing the failure.

The results obtained from the ILSS of the CF/PA6 composites are shown in Figure 3-D. It is observed that the values of the samples before and after exposure to accelerated weathering are close, 27.2 MPa (± 0.9 MPa), without statistical differences. However, the CF/PA6 composites after being exposed to accelerated weathering for 400 h and 1200 h showed a slight increase of 0.4% and 3.1%, respectively, in the mean resistance values of ILSS when compared to the unconditioned composite. This behavior suggests that the exposure time which may have promoted an improvement in the fiber/matrix interface of the composites, but this behavior needs to be further investigated.

After ILSS tests, OM analyses were carried out to analyze the failure mode resulted from the ILSS tests. The images obtained from the fracture region are shown in Figure 5. The fracture of the tested specimens occurred in the central region of the transversal face of the specimen, as expected for the ILSS tests. First, the analysis of these images shows a homogeneous distribution of matrix and fibers in the laminate. The unconditioned CF/PA6 composite showed numerous intralaminar fractures in the CF cables at 0º and interlaminar fractures (highlighted in yellow) along the analyzed surface. This type of failure generally tends to fracture in the plane of the laminate, oriented between layers, and results mainly in the fracture of the polymeric matrix with a few exceptions that can fracture the fibers.

CF/PA6 composites after 400 h, 800 h, and 1200 h exposed to accelerated weathering showed more interlaminar, intralaminar, and translaminar fractures. The presence more intense of these three types of fractures may be related to a possible fragility of the polymeric matrix, as they are exposed to accelerated weathering, with the presence of UV

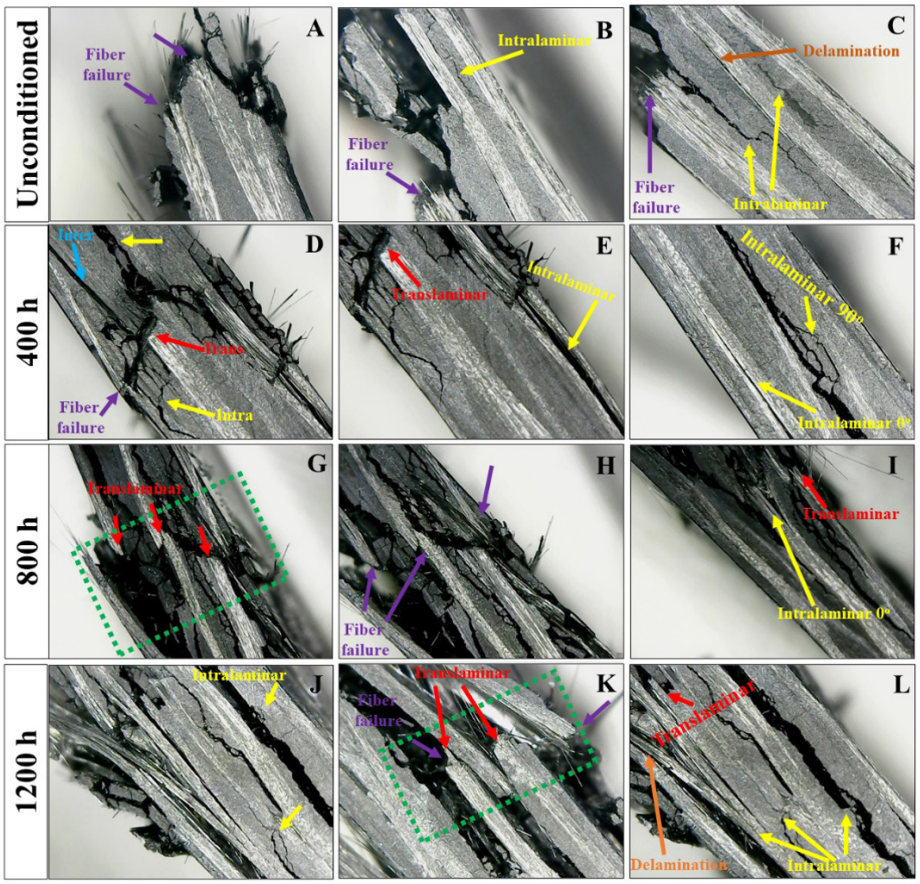

Figure 4. Representative macroscopic images of tensile fracture surface from the CF/PA6 composites unconditioned and after 400 h, 800 h, and 1200 h exposed to accelerated weathering.

radiation, humidity, and temperature. These factors may have influenced the beginning of matrix degradation. The matrix suffered intralaminar fractures, followed by interlaminar fractures, followed by translaminar fractures, which occur transversely to the plane of the laminate, causing the fiber breakage (highlighted in green).

Figure 6 presents SEM images of the surface of the specimens after exposure at different times in accelerated weathering. No change in the color of the composites was observed after this degradative process. Since the depth of penetration of UV radiation is small, resulting in surface degradation mainly by surface grooves (highlighted in yellow), which can lead to embrittlement of the matrix and the formation of microcracks. This behavior was more pronounced in the CF/PA6 composites after 800 h and 1200 h of exposure, and some regions with signs of erosion followed by the presence of some holes and cavitations (highlighted with red arrows).

Furthermore, since UV radiation affects the surface of materials and causes changes in surface morphology, prolonged exposure to UV radiation can deteriorate the surface, and consequently form surface defects where moisture, environmental pollutants, and other factors can migrate to the interior of components. Then, it can start a degradative process of the material and can result in the deterioration and decrease of the mechanical resistance, for example, and even the premature failure of some components in use[8,12].

Consequently, with the increase in the exposure time to accelerated weathering the surface degradation is intensified causing an increase in the surface wettability value. This effect can result in high moisture absorption by the composite as shown in the contact angle presented in Figure 7. The contact angle measurements were done using the distilled water drop. The values < 90º and > 90º correspond to hydrophilic and hydrophobic surfaces, respectively. The unconditioned CF/PA6 composite presents a contact angle value of 82º, and after 400 h, 800 h, and 1200 h of exposure to the accelerated weathering, these values decreased to 62º, 57º, and 52º, respectively, that is, after conditioning the material became more hydrophilic, favoring the wettability and, consequently, the moisture absorption.

The approximately 30% reduction in contact angle values suggests that the UV radiation, together with other factors present in the accelerated weathering chamber, such as humidity and temperature, strongly affected the composite surface. This behavior was also observed by Mahat et al.[31], who submitted CF/PPS composites to 120, 240, 360, and 480 h of UV radiation, and suggested that the reduction in contact angle values also implied in the surface erosion mechanism, in addition to an increase in

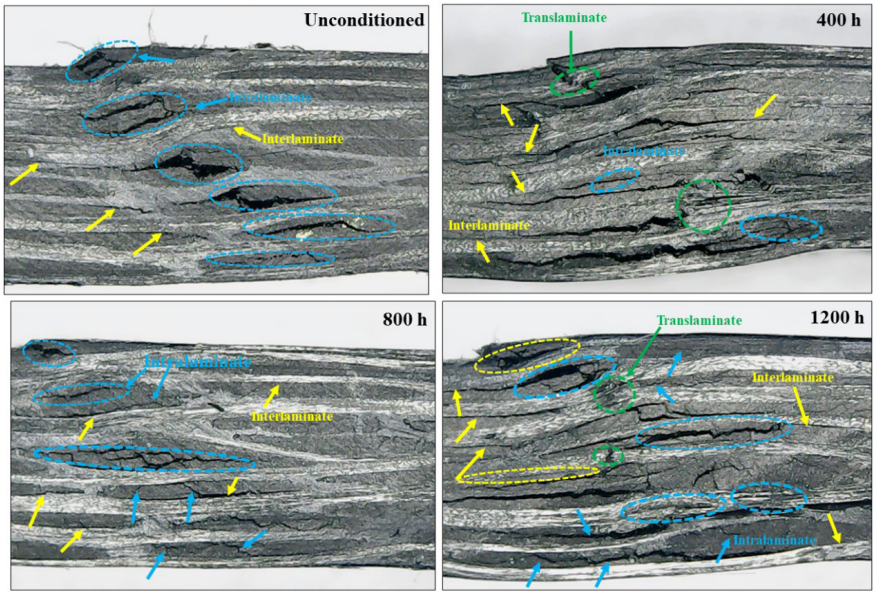

Figure 5. MO of ILSS fracture of CF/PA6 composite unconditioned and after 400 h, 800 h, and 1200 h exposed to accelerated weathering.

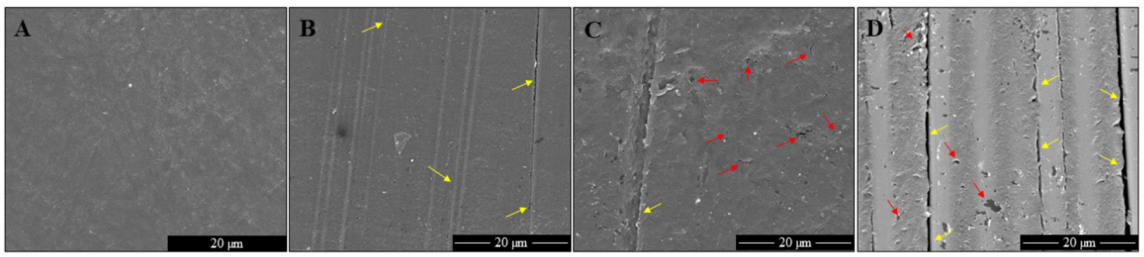

Figure 6. SEM images of the degraded surface after exposure to 0h (A), 400 h (B), 800 h (C), and 1200 h (D) in an accelerated weathering environment, 5,000x.

the wettability of the composites, leading to high moisture absorption and, consequently, greater degradation of the material.

Figure 8 shows SEM micrographs of the tensile fracture of the CF/PA6 composites after exposure to 400 h, 800 h, and 1200 h in an accelerated weathering environment. In general, in all micrographs of the composites after exposure to accelerated weathering, it is observed that the fiber-matrix interface was preserved, maintaining the structural integrity of the specimens. Furthermore, as seen in the surface micrographs of the composites (Figure 6), few signs of surface degradation were observed, indicating that the exposure times studied resulted in early morphological degradation of the composites. Similar behavior was observed by Pillay, Vaidya, and Janowski[35], who submitted CF/PA6 composites at 100, 200, 300, 420, and 600 h at only UV exposure, without the combination of other factors, such as temperature and humidity. Therefore, the present work used a longer period of exposure in addition to the combination of factors such as UV radiation, humidity, and temperature, which is more aggressive, and even so, we observed behavior similar to that of the authors[35].

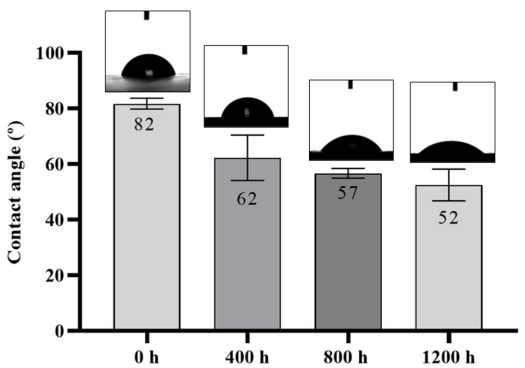

Figure 7. Contact angle measurements and distilled water drop image: CF/PA6 composites before and after the exposure times of 400 h, 800 h, and 1200 h in accelerated weathering.

In the images of the unconditioned composites (Figure 8-A-B-C) it is possible to observe delamination (Figure 8-A), regions of broken fibers (Figure 8-B), and the plastic deformation of the matrix, as well as the good adhesion of the matrix in the CF (Figure 8-C).

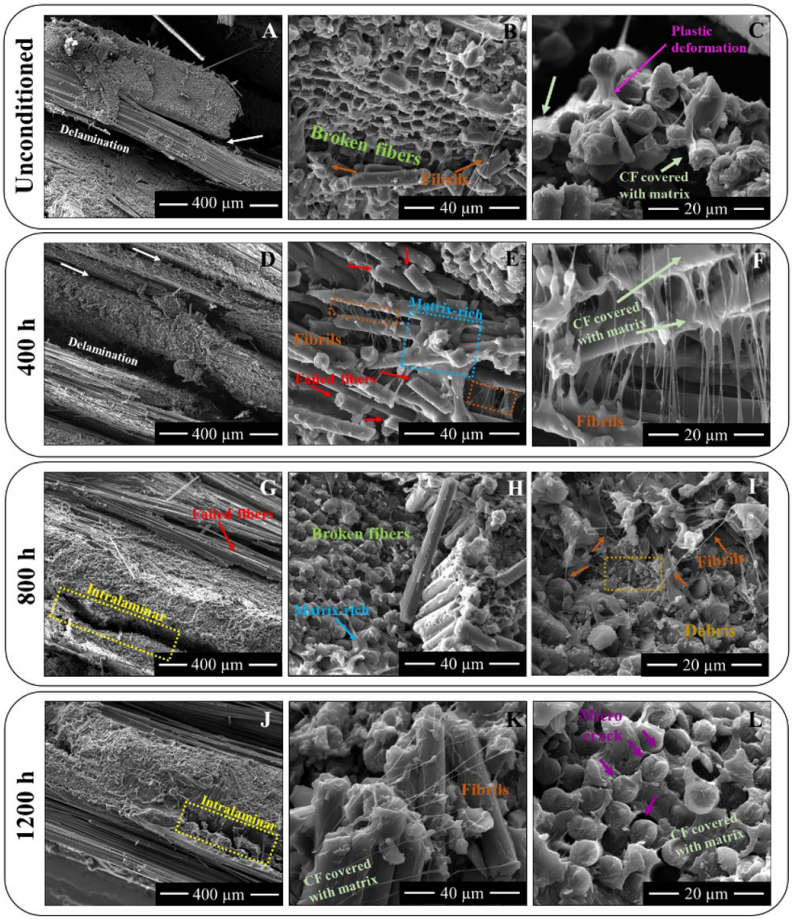

Figure 8. Fractography aspects of CF/PA6 composites: unconditioned (500x A, 2,500x B, and 5,000x C), after 400 h (500x D, 2,500x E, and 5,000x F), 800h (500x G, 2,500x H, and 5,000x I), and 1200 h (500x J, 2,500x K, and 5,000x L) exposed to accelerated weathering.

In the images of CF/PA6 composites after different exposure times to accelerated weathering, it is possible to visualize the integrity of the matrix and reinforcement, with the presence of delamination, intralaminar fractures and ruptured CF, typical of tensile fractures (Figure 8 D-G-J). In addition to the presence of plastic deformation by the matrix and by the fibrils, as well as the good adhesion of the matrix to the CF, indicates CF is covered with the PA6 matrix.

However, when comparing the micrographs of the unconditioned composites and after 400 h, 800 h, and 1200 h exposed to accelerated weathering, it is possible to observe that the unconditioned composite shows the CF well adhered and coated by the matrix (Figure 8-C). In the images of the composites after the accelerated weathering, smoother CF can be observed, with less PA6 matrix adhered to their surfaces, in addition to more pulled fibers due to the detachment of the matrix, forming micro-cracks. This behavior is more evident in the composites after 1200 h of exposure (Figure 8-L), since in this exposure time the deterioration of the matrix may have started, and consequently the detachment of the interface.

4. Conclusions

This work presented the influence of various weathering conditions, such as UV radiation, temperature, and humidity, at different exposure times (400 h, 800 h, and 1200 h) on the thermal, structural, and mechanical properties of CF/PA6 composites. The conditioning times studied did not significantly influence the thermal stability of the composites, with no changes being observed in the T_m and only a slight variation in the X_c values. The polymeric matrix was preserved, without major signs of degradation, just some cracks and the beginning of erosion points, which were indicated by SEM images and FT-IR spectra. Thus, the resistance to ILSS, which is dominated by the matrix, did not show statistical differences, as well as the tensile strength, which is dominated by reinforcement, also did not show statistical differences. And so, through micrographs of the tensile fracture, it was possible to confirm the internal preservation of the composites, without evidence of matrix and reinforcement degradation. These results confirm that thermoplastic matrix composites can be used in lightweight external structural applications, without major losses in their properties and may be an alternative to the use of thermoset matrices.

5. Author's Contribution

• **Conceptualization** – Larissa Stieven Montagna; Mirabel Cerqueira Rezende.

• **Data curation** – Larissa Stieven Montagna; Mirabel Cerqueira Rezende.

• **Formal analysis** – Larissa Stieven Montagna; Guilherme Ferreira de Melo Morgado; Mirabel Cerqueira Rezende.

• **Funding acquisition** – Mirabel Cerqueira Rezende; Alessandro Guimarães.

• **Investigation** – Larissa Stieven Montagna; Guilherme Ferreira de Melo Morgado; Mirabel Cerqueira Rezende.

• **Methodology** – Larissa Stieven Montagna; Mirabel Cerqueira Rezende.

• **Project administration** – Mirabel Cerqueira Rezende.

• **Resources** – Fabio Roberto Passador; Juliano Marini; Mirabel Cerqueira Rezende.

• **Software** – NA.

• **Supervision** – Mirabel Cerqueira Rezende.

• **Validation** – Fabio Roberto Passador; Mirabel Cerqueira Rezende.

• **Visualization** – Larissa Stieven Montagna; Mirabel Cerqueira Rezende.

• **Writing – original draft** – Larissa Stieven Montagna; Guilherme Ferreira de Melo Morgado; Juliano Marini; Thaís Larissa do Amaral Montanheiro; Alessandro Guimarães; Fabio Roberto Passador; Mirabel Cerqueira Rezende.

• **Writing – review & editing** – Larissa Stieven Montagna; Guilherme Ferreira de Melo Morgado; Juliano Marini; Thaís Larissa do Amaral Montanheiro; Alessandro Guimarães; Fabio Roberto Passador; Mirabel Cerqueira Rezende.

6. Acknowledgements

The authors would like to thank the CNPq processes 305123/2018-1 and 307933/2021-0) for the financial support, and the Federal Government Program 'Rota 2030' linked to the "Development of Skills for Design and Manufacturing of Tooling for Composite Parts" n° 27194.03.03/2020.01-00 for the financial support; the Lightweight Structures Laboratory from IPT for the coordination, and also the Brazilian Funding Institutions FIPT for the administrative support.

7. References

1. Alshammari, B. A., Alsuhybani, M. S., Almushaikeh, A. M., Alotaibi, B. M., Alenad, A. M., Alqahtani, N. B., & Alharbi, A. G. (2021). Comprehensive review of the properties and modifications of carbon fiber-reinforced thermoplastic composites. *Polymer*, *13*(15), 2474. http://dx.doi.org/10.3390/polym13152474. PMid:34372077.
2. Montagna, L. S., Morgado, G. F. M., Lemes, A. P., Passador, F. R., & Rezende, M. C. (2002). Recycling of carbon fiber-reinforced thermoplastic and thermoset composites: a review. *Journal of Thermoplastic Composite Materials*, *36*(8), 3455-3480. http://dx.doi.org/10.1177/08927057221108912.
3. American Institute of Aeronautics and Astronautics. (2023). *Buckling tolerance design of aircraft fuselage using carbon fiber reinforced thermoplastic (CFRTP).* USA: American Institute of Aeronautics and Astronautics, Inc.
4. Goh, G. D., Toh, W., Yap, Y. L., Ng, T. Y., & Yeong, W. Y. (2021). Additively manufactured continuous carbon fiber-reinforced thermoplastic for topology optimized unmanned aerial vehicle structures. *Composites. Part B, Engineering*, *216*, 108840. http://dx.doi.org/10.1016/j.compositesb.2021.108840.
5. Sarfraz, M. S., Hong, H., & Kim, S. S. (2021). Recent developments in the manufacturing technologies of composite components and their cost-effectiveness in the automotive industry: areview study. *Composite Structures*, *266*, 113864. http://dx.doi.org/10.1016/j.compstruct.2021.113864.
6. Thomas, L., & Ramachandra, M. (2018). Advanced materials for wind turbine blade: a review. *Materials Today: Proceedings*, *5*(1), 2635-2640. http://dx.doi.org/10.1016/j.matpr.2018.01.043.
7. Wang, F. (2021). Application of new carbon fiber material in sports equipment. *IOP Conference Series. Earth and Environmental Science*, *714*(3), 032064. http://dx.doi.org/10.1088/1755-1315/714/3/032064.
8. Ray, S., & Cooney, R. P. (2018). *Thermal Degradation of Polymer and Polymer Composites.* In M. Kutz (Ed.), *Handbook of environmental degradation of materials* (pp. 185-206). India: William Andrew. http://dx.doi.org/10.1016/B978-0-323-52472-8.00009-5
9. Sang, L., Wang, Y., Wang, C., Peng, X., Hou, W., & Tong, L. (2019). Moisture diffusion and damage characteristics of carbon fabric reinforced polyamide 6 laminates under hydrothermal aging. *Composites. Part A, Applied Science and Manufacturing*, *123*, 242-252. http://dx.doi.org/10.1016/j.compositesa.2019.05.023.
10. Afshar, A., Alkhader, M., Korach, C. S., & Chiang, F. (2015). Effect of long-term exposure to marine environments on the flexural properties of carbon fiber vinylester composites. *Composite Structures*, *126*, 72-77. http://dx.doi.org/10.1016/j.compstruct.2015.02.008.
11. Pavlenko, V. I., Zabolotny, V. T., Cherkashina, N. I., & Edamenko, O. D. (2014). Effect of vacuum ultraviolet on the surface properties of high-filled polymer composites. *Inorganic Materials: Applied Research*, *5*(3), 219-223. http://dx.doi.org/10.1134/S2075113314030137.
12. Ching, Y. C., Gunathilake, T. M. S. U., Ching, K. Y., Chuah, C. H., Sandu, V., Singh, R., & Liou, N. (2019). *Effects of high temperature and ultraviolet radiation on polymer composites.* In M. Jawaid, M. Thariq, & N. Saba (Eds.), *Durability and life prediction in biocomposites, fibre-reinforced composites and hybrid composites* (pp. 407-426). UK: Woodhead Publishing. http://dx.doi.org/10.1016/B978-0-08-102290-0.00018-0
13. Awaja, F., Nguyen, M.-T., Zhang, S., & Arhatari, B. (2011). The investigation of inner structural damage of UV and heat degraded polymer composites using X-ray micro–CT. *Composites. Part A, Applied Science and Manufacturing*, *42*(4), 408-418. http://dx.doi.org/10.1016/j.compositesa.2010.12.015.
14. Chin, J. W. (2007). *Durability of composites exposed to ultraviolet radiation. Durability of Composites for Civil Structural Applications.* In V. M. Karbhari (Ed.), *Durability of composites for civil structural applications* (pp. 80-97). UK: Woodhead Publishing Limited. http://dx.doi.org/10.1533/9781845693565.1.80
15. Troughton, M. J. (2009). *Polyamides.* In M. J. Troughton (Ed.), *Handbook of plastics joining: a practical guide* (pp. 251-281). USA: William Andrew Inc. http://dx.doi.org/10.1016/B978-0-8155-1581-4.50027-5
16. Kondo, M. Y., Montagna, L. S., Morgado, G. F. M., Castilho, A. L. G., Batista, L. A. P. S., Botelho, E. C., Costa, M. L., Passador, F. R., Rezende, M. C., & Ribeiro, M. V. (2022).

Recent advances in the use of Polyamide-based materials for the automotive industry. *Polímeros Ciência e Tecnologia*, *32*(2), e2022023. http://dx.doi.org/10.1590/0104-1428.20220042.

17. Kroes, G. H. (1963). The photo-oxidation of nylon 6 and 66. *Recueil des Travaux Chimiques des Pays-Bas (Leiden, Netherlands)*, *82*(10), 979-987. http://dx.doi.org/10.1002/recl.19630821006.
18. McK, J. F. (1976). Photodegradation, photo-oxidation and photostabilization of polymers: B. Ranby and J.F. Rabek, John Wiley, London, New York, Sydney and Toronto, 1975, pp. xv + 573, price £16.50. *Journal of Molecular Structure*, *33*(1), 152-153. http://dx.doi.org/10.1016/0022-2860(76)80158-5.
19. Ishak, Z. A. M., & Berry, J. P. (1994). Hygrothermal aging studies of short carbon fiber reinforced nylon 6.6. *Journal of Applied Polymer Science*, *51*(13), 2145-2155. http://dx.doi.org/10.1002/app.1994.070511306.
20. Lei, Y., Zhang, T., Zhang, J., & Zhang, B. (2021). Dimensional stability and mechanical performance evolution of continuous carbon fiber reinforced polyamide 6 composites under hygrothermal environment. *Journal of Materials Research and Technology*, *13*, 2126-2137. http://dx.doi.org/10.1016/j.jmrt.2021.06.012.
21. Sang, L., Wang, C., Wang, Y., & Hou, W. (2018). Effects of hydrothermal aging on moisture absorption and property prediction of short carbon fiber reinforced polyamide 6 composites. *Composites. Part B, Engineering*, *153*, 306-314. http://dx.doi.org/10.1016/j.compositesb.2018.08.138.
22. Pinpathomrat, B., Yamada, K., & Yokoyama, A. (2020). The efect of UV irradiation on polyamide 6/carbon-fber composites based on three-dimensional printing. *SN Applied Sciences*, *2*(9), 1518. http://dx.doi.org/10.1007/s42452-020-03319-4.
23. Montagna, L.S., Morgado, G.F.M., Santos, L.F.P., Guimarães, A., Passador, F.R., & Rezende, M.C. (2023). Mechanical performance of carbon fiber/polyamide 6: comparative study between conditioning in distilled water with heating and saline solution. *Materials Research*, In press.
24. Khanna, Y. P., & Kuhn, W. P. (1997). Measurement of crystalline index in nylons by DSC: complexities and recommendations. *Journal of Polymer Science. Part B, Polymer Physics*, *35*(14), 2219-2231. http://dx.doi.org/10.1002/(SICI)1099-0488(199710)35:14<2219::AID-POLB3>3.0.CO;2-R.
25. American Society for Testing and Materials – ASTM. (2008). *ASTM D3039/D3039M-08: standard test method for tensile properties of polymer matrix composite materials*. West Conshohocken: ASTM.
26. American Society for Testing and Materials – ASTM. (2013). *ASTM D2344/D2344M-13: standard test method for short-beam strength of polymer matrix composite materials and their laminates*. West Conshohocken: ASTM.
27. Hein, L. R. O., Campos, K. A., Caltabiano, P. C. R. O., & Kostov, K. G. (2013). A brief discussion about image quality and SEM methods for quantitative fractography of polymer composites. *Scanning*, *35*(3), 196-204. http://dx.doi.org/10.1002/sca.21048. PMid:22915360.
28. Fernández-Rosas, E., Pomar-Portillo, V., González-Gálvez, D., Vilar, G., & Vázquez-Campos, S. (2020). Release mechanisms for PA6 nanocomposites under weathering conditions simulating their outdoor uses. *NanoImpact*, *20*, 100260. http://dx.doi.org/10.1016/j.impact.2020.100260.
29. Batista, N. L., Faria, M. C. M., Iha, K., Oliveira, P. C., & Botelho, E. C. (2013). Influence of water immersion and ultraviolet weathering on mechanical and viscoelastic properties of polyphenylene sulfide– carbon fiber composites. *Journal of Thermoplastic Composite Materials*, *28*(3), 340-356. http://dx.doi.org/10.1177/0892705713484747.
30. Lim, L., Britt, I. J., & Tung, M. A. (1999). Sorption and transport of water vapor in nylon 6,6 film. *Journal of Applied Polymer Science*, *71*(2), 197-206. http://dx.doi.org/10.1002/(SICI)1097-4628(19990110)71:2<197::AID-APP2>3.0.CO;2-J.
31. Oulidi, O., Nakkabi, A., Elaraaj, I., Fahim, M., & El Moualij, N. (2022). Incorporation of olive pomace as a natural filler in to the PA6 matrix: effect on the structure and thermal properties of synthetic Polyamide 6. *Chemical Engineering Journal Advances*, *12*, 100399. http://dx.doi.org/10.1016/j.ceja.2022.100399.
32. Mahat, K. B., Alarifi, I., Alharbi, A., & Asmatulu, R. (2016). Effects of UV light on mechanical properties of carbon fiber reinforced PPS thermoplastic composites. *Macromolecular Symposia*, *365*(1), 157-168. http://dx.doi.org/10.1002/masy.201650015.
33. Mazur, R. L., Oliveira, P. C., Rezende, M. C., & Botelho, E. C. (2014). Environmental effects on viscoelastic behavior of carbon fiber/PEKK thermoplastic composites. *Journal of Reinforced Plastics and Composites*, *33*(8), 749-757. http://dx.doi.org/10.1177/0731684413515955.
34. Godara, A., Raabe, D., & Green, S. (2007). The influence of sterilization processes on the micromechanical properties of carbon fiber-reinforced PEEK composites for bone implant applications. *Acta Biomaterialia*, *3*(2), 209-220. http://dx.doi.org/10.1016/j.actbio.2006.11.005. PMid:17236831.
35. Pillay, S., Vaidya, U. K., & Janowski, G. M. (2009). Effects of moisture and UV exposure on liquid molded carbon fabric reinforced nylon 6 composite laminates. *Composites Science and Technology*, *69*(6), 839-846. http://dx.doi.org/10.1016/j.compscitech.2008.03.021.

Received: July 10, 2023
Revised: Aug. 30, 2023
Accepted: Sept. 04, 2023